An Adaptive Upper-Arm EMG-Based Robot Control System

Hsiu-Jen Liu and Kuu-Young Young

Abstract

The human-assisting robot can be helpful for improving the life quality of the disabled and elderly. As Electromyography (EMG) is a physiological signal generated during muscle contraction, it implicates, to certain extent, the human intention for movement, and is thus very suitable to serve as the control signal for the assisting robot. In this paper, we develop an upper-arm EMG-based robot control system, which provides a natural and intuitive manipulation. To satisfy the demand of real-time control, we propose a simple and effective method for the mapping between the upper-arm EMG signal and corresponding movement. However, due to the fuzziness inherent in the EMG signals, which are time-varying and highly nonlinear, the tuning for system parameters is not that straightforward. We therefore employ the concept of fuzzy system to find proper parameters that better suit for the individual users. To provide better adaptive capability, we propose using the adaptive neuro-fuzzy inference system (ANFIS) to realize the fuzzy system. We perform a series of experiments to demonstrate the effectiveness of the proposed adaptive upper-arm EMG-based robot control system.

Keywords: Adaptive neuro-fuzzy inference system, Electromyography (EMG) signal, Human-assisting robot.

1. Introduction

Nowadays, the number of disabled and elderly is increasing. With a decreasing birthrate, the development of the human-assisting robot is imperative for them to alleviate the dependence and improve the quality of life. Teach box, joystick, and keyboard, are traditional devices used for robot manipulation. Currently, voice control also becomes an alternate [1]. Meanwhile, Electromyography signal, as a physiological signal generated during muscle contraction, is also adopted for the manipulation of the rehabilitation device. EMG signal reflects the muscular force level, and consequently the human intention for movement. As it leads to a more natural and intuitive manipulation, EMG is very suitable to serve as the control signal. Researches have been devoted for applying the EMG signal for robot motion governing. Fukuda et al. [2] proposed teleoperating a human-assisting manipulator by using EMG signals. Artemiadis and Kyriakopoulos [3] proposed an EMG-based position and force control scheme for robot arm. Ferreira et al. [4] applied the EMG and EEG for developing the interfaces for robot systems. Gao et al. [5] developed a robotic arm wrestling system based on EMG and artificial neural network. And, Gopura and Kiguchi [6] developed exoskeleton robots for assisting the motion of physically weak individuals based on EMG and fuzzy control.

Among these researches, EMG signals were identified to be affected by noises, such as ECG crosstalk, electromagnetic induction from power lines, and arm and cable movements. Meanwhile, muscle mutual interference, physiological condition (e.g., fatigue), skin impedance, etc., also contribute to the fuzziness of the EMG signals, which are time-varying and highly nonlinear. These EMG properties much increase the difficulty in extracting proper EMG features for motion classification. Some researchers proposed using the learning approach, e.g., the neural network [5,7-8], and reported salient performance. However, the learning approach demands certain computational load and incurs some system complexity for the learning and training processes involved. In this paper, we propose an initial point detection method [9], which can effectively establish the relationship between the upper-arm EMG signals and corresponding movements. The proposed method does not involve complicated computation nor training and learning processes. However, system parameters need to be tuned to adapt to the status of the individual user. To tackle it, we propose using the concept of the fuzzy system, so that the tedious process encountered in the trial and error method can be avoided. For its excellence on adaptation, we employ the adaptive neuro-fuzzy inference system (ANFIS) [10-13] to realize the fuzzy system. The ANFIS has been successfully implemented in biomedical engineering for classification [14-17] and robot control [18-19]. To demonstrate the

Corresponding Author: Kuu-Young Young is with the Department of Electrical Engineering, National Chiao Tung University, 1001 University Road, Hsinchu, Taiwan 300.
E-mail: kyoung@mail.nctu.edu.tw
Manuscript received 16 Nov. 2009; revised 15 Apr. 2010; accepted 9 June. 2010.

effectiveness of the proposed approach, a series of experiments are performed.

The rest of the paper is organized as follows. Section 2 describes the proposed upper-arm EMG-based robot control system, including the modules for EMG signal measurement and processing, feature extraction, and motion classification with adaptation. Section 3 presents the experimental results. And, Section 4 gives the conclusion.

2. Proposed Upper-Arm EMG-Based Robot Control System

Figure 1 shows the system diagram of the proposed upper-arm EMG-based robot control system, which consists of three main modules: signal measurement and processing, feature extraction, and motion classification with adaptation. The signal measurement and processing module measures the raw EMG signals and also filters out the noises. The filtered EMG signals are then sent to the feature extraction module to derive their features. With the extracted features, the motion classification with adaptation module determines the corresponding arm movements and generates the commands to drive the human-assisting robot. From the resultant robot motion, the operator evaluates the performance and determines next movement. These three modules are described below.

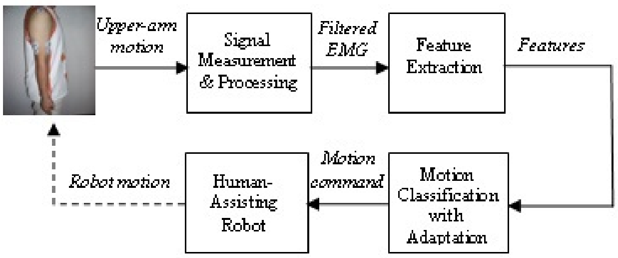

Figure 1. Proposed upper-arm EMG-based robot control system.

A. *Signal Measurement and Processing*

For EMG signal measurement, we need to consider the locations and areas on those muscles involved during upper-arm movement. We focus on the EMG signals of the primary flexor and extensor muscles, i.e., Biceps Brachii and Triceps Brachii, respectively. The measurement also depends on the regions where the electrodes are placed. To obtain more precise EMG signals, the electrodes need to be placed on the belly of the muscle. Several types of noises may affect the measurement of the EMG signals, such as ECG crosstalk, electromagnetic induction from power lines, and arm and cable movements. The ECG crosstalk can be suppressed by measuring signals from those muscles away from the heart. The frequency of the electromagnetic noise is around 60 Hz, which is within the primary frequency of the EMG signal (50~150 Hz). Therefore, the band-rejection filter is not suggested for its removal. Meanwhile, the frequency distribution for the arm and cable movements is around 0 to 20 Hz, which can be tackled using a high-pass filter.

B. *Feature Extraction*

Four famous feature extraction indices, mean absolute value (MAV), variance (VAR), bias zero-crossing (BZC), and Willison amplitude (WAMP) are frequently used to extract the EMG signals. The formulae for these indices are listed in Table 1, in which X_k denotes the *k*th sampling data in the window for computing the feature and *N* is the window length. MAV is taken as a signal power estimator and VAR that for power density. Both MAV and VAR are frequently used to estimate the contraction level of the muscle. BZC, which includes a bias value for dealing with background noise or disturbance, counts the zero-crossing, i.e., the number of times the signal passes a biased zero, thus providing frequency information of the EMG signal. And, WAMP, that counts the number of times that the signal amplitude exceeds a predefined threshold, serves as an indicator of the contraction level of the muscle. The proposed method adopts MAV as the feature extraction index, because we intend to evaluate the contraction level of the muscle. Meanwhile, VAR can also be an alternative.

Table 1. Feature extraction indices and formulae.

Name	Formula
MAV	$MAV = \frac{1}{N}\sum_{k=1}^{N}\lvert X_k \rvert$
VAR	$VAR = \frac{1}{N-1}\sum_{k=1}^{N} X_k{}^2$
BZC	$BZC = \sum_{k=1}^{N}\mathrm{sgn}\left[(X_k - 0.4)\times(X_{k-1} - 0.4)\right]$ $\mathrm{sgn}(x) = \begin{cases} 1 \text{ , if } x > 0 \\ 0 \text{ , others} \end{cases}$
WAMP	$WAMP = \sum_{k=1}^{N} f(\lvert X_k - X_{k-1} \rvert);$ $f(x) = \begin{cases} 1 \text{ , if } \; x > threshold \\ 0 \text{ , if otherwise} \end{cases}$

C. *Motion Classification with Adaptation*

To achieve real-time motion classification, we propose an initial point detection method to deduce the motion intention from the EMG signal [9]. This method determines the onset of the upper arm motion via detecting the instant when the magnitude of the extracted EMG feature reaches the critical values.

From the observation, muscle states exhibit fluctuations during both relaxation and flexion. Figure 2 shows an example, in which MAV is used to evaluate the EMG signal of Biceps Brachii. In Figure 2, section A indicates the muscle state during relaxation, and section B that during flexion, both of which exhibit some fluctuations. We thus propose a concept of double critical value detection, as illustrated in Figure 3 [9]. In Figure 3, the state of the muscle *MS* is determined to be active when the initial value for the feature F_k is larger than the upper critical value CV_u, and *MS* inactive when F_k is smaller than the lower critical value CV_l. And, an active *MS* corresponds to an "ON'' robot command and an inactive one for that of "OFF''. This relationship can be formulated as

$$MS = \begin{cases} 1, & if \quad F_k > CV_u \\ 0, & if \quad F_k < CV_l \end{cases} \tag{1}$$

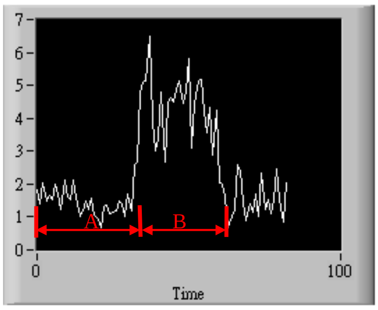

Figure 2. EMG signal evaluation of Biceps Brachi using MAV (Horizontal coordinate: Time (second), Vertical coordinate: Amplitude (voltage)).

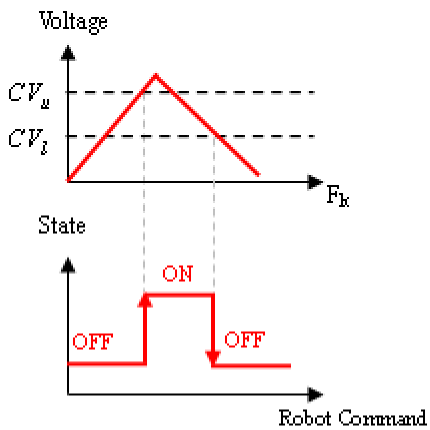

Figure 3. Conceptual diagram for double critical value detection.

The selection of CV_u and CV_l is very critical for the performance of the motion classifier. A high CV_u implies that the user has to generate a larger force to move the robot arm. It may lead to muscle fatigue, in addition to the increase of the crosstalk between muscles. On the contrary, a small CV_u results in low tolerance against the noise. Meanwhile, a large CV_l may make the robot arm stop its movement earlier than that of the user, while a small CV_l lead to the opposite. Their selection is user-dependent. For finding proper CV_u and CV_l, we first utilize the empirical knowledge to generate the fuzzy rules, listed in Table 2, where MAV (time-domain estimation) and BZC (frequency-domain estimation) are the input variables, CV_u (CV_l) the output variable, W, M, and S stand for weak, middle, and strong, and L, M, and H for low, middle, and high. We then employ the ANFIS for automatic parameter tuning. Figure 4 shows the conceptual diagram of the proposed ANFIS, in which the IF-THEN rules are formulated as

R^i: *IF* MAV *is* A_i *and* BZC *is* B_i *THEN* CV_u $(CV_l)_i$, = p_i ·MAV + q_i ·BZC + r_i, $i \in \{1,2, \cdots, 9\}$ (2)

where A, B = {W, M, S} are linguistic variables, and $[p_i \quad q_i \quad r_i]$ the consequent parameter set, determined by the least square method.

The proposed ANFIS consists of five layers, as shown in Figure 5. Layer 1 is the input layer. Each node in this layer represents an input variable of the model with the membership function:

$$O_i^1 = \mu_{A_i}(MAV), \quad O_{i+3}^1 = \mu_{B_i}(BZC), \quad i = 1,2,3 \tag{3}$$

The bell-shaped membership function is employed, shown in Figure 6, and expressed as

$$\mu_{A_i}(MAV) = \frac{1}{1 + \left\{ \left[(MAV - c_i) / a_i \right]^2 \right\}^{b_i}}, \quad i = 1,2,3 \tag{4}$$

$$\mu_{B_i}(BZC) = \frac{1}{1 + \left\{ \left[(BZC - c_i) / a_i \right]^2 \right\}^{b_i}}, \quad i = 1,2,3 \tag{5}$$

where $[a_i \quad b_i \quad c_i]$ represents the premise parameter set, which can be determined by the backpropagation gradient descent method. Layer 2 is the inference layer. Each node in this layer is multiplied by the input signals to become w_i, the firing strength of the rule:

$$O_i^2 = w_i = \mu_{A_i}(MAV) \times \mu_{B_i}(BZC), \quad i = 1,2,\cdots,9 \tag{6}$$

Layer 3 is the normalization layer that normalizes the firing strength by calculating the ratio of i^{th} firing strength to their sum:

$$O_i^3 = \overline{w}_i = \frac{w_i}{\sum_{i=1}^{9} w_i}, \quad i = 1,2,\cdots,9 \tag{7}$$

Layer 4 is the output layer. Each node multiplies the normalized firing strength by the consequent function to generate the qualified consequent of each rule. The output of the node is computed as

$$O_i^4 = \overline{w}_i CV_u (CV_l)_i = \overline{w}_i (p_i \cdot MAV + q_i \cdot BZC + r_i), \quad i = 1,2,\cdots,9 \tag{8}$$

Layer 5 is the defuzzification layer, which computes the weighted average of the output signals from the output layer:

$$O_i^5 = \sum_{i=1}^{9} \overline{w}_i CV_u\left(CV_l\right)_i = \frac{\sum_{i=1}^{9} w_i CV_u\left(CV_l\right)_i}{\sum_{i=1}^{9} w_i} \quad (9)$$

Table 2. Fuzzy rule base.

CV_u (CV_l)		BZC W	BZC M	BZC S
MAV	W	***L***	***L***	***L***
	M	***L***	***M***	***M***
	S	***L***	***H***	***H***

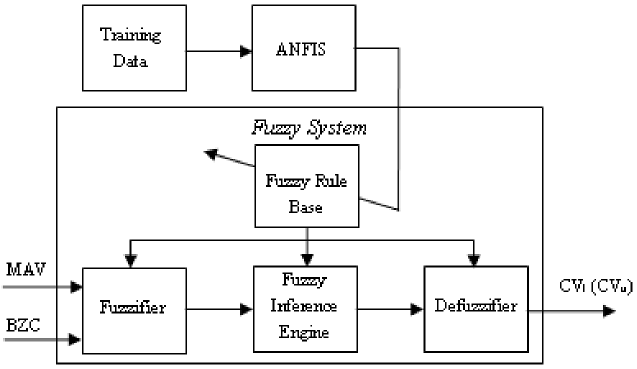

Figure 4. Conceptual diagram of the proposed ANFIS for CV_u and CV_l determination.

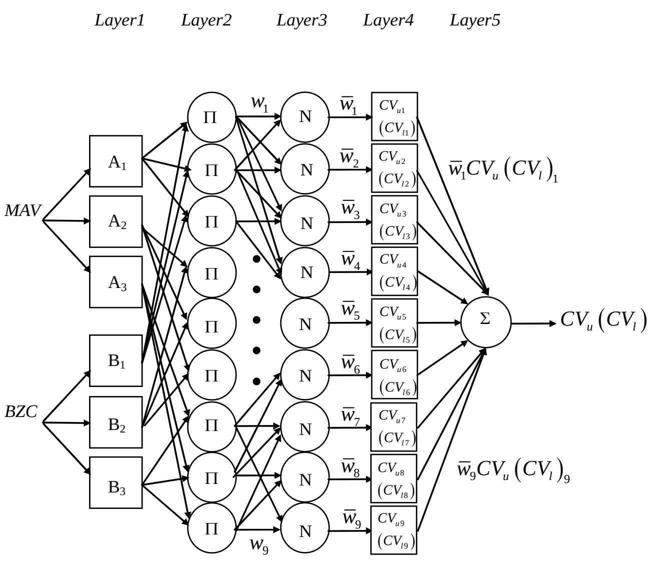

Figure 5. Structure of the ANFIS for the proposed system.

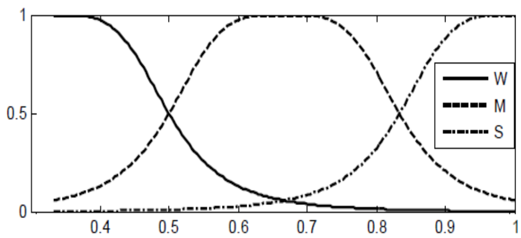

Figure 6. Bell-shaped membership functions for input variables.

3. Experiments

In the experiments, we applied the proposed system for robot motion governing based on the measured upper-arm EMG signals. Figure 7 shows the implementation of the proposed system for experiments. In Figure 7, the measured EMG signals are first amplified using the ETH-256 physiological signal amplifier (manufactured by iWorx Systems, USA), and the amplified analog signals then transformed into digital signals via National Instrument USB-6009 A/D data acquisition device (with 1 KHz sampling rate). The digital signals are further forwarded to the LabVIEW development system, which includes a sixth-order band-pass Butterworth filter (with the cut-off frequencies at 20 and 400 Hz, respectively), a 10-sampling-data-window feature extractor, an initial point detector and ANFIS, and a motion classifier. Via the processing, motion commands are determined and sent to a 6-DOF (degree of freedom) Mitsubishi RV-2A robot arm for execution (with only link three manipulated). Two sets of electrodes are placed on the Biceps Brachii, marked as CH1+/-, and the Triceps Brachii, marked CH2+/-, respectively. When EMG signals from both CH1 and CH2 are determined to be OFF, the classifier outputs 0 as relaxation; ON for CH1 and OFF for CH2, outputs 1 as flexion; OFF for CH1 and ON for CH2, outputs 2 as extension; and ON for CH1 and ON for CH2, outputs 3 as error detection. Table 3 summarizes the mapping from EMG to robot movement. For performance evaluation, we define the successful discrimination rate (SDR) as the times that the robot arm follows the motion of the subject's upper arm correctly out of the total number of classification:

$$SDR = \frac{\text{Number of successful motion following}}{\text{Total number of classification}} \times 100\% \quad (10)$$

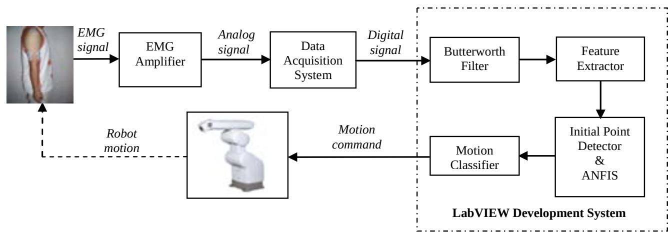

Figure 7. Implementation of the proposed system for experiments.

Two male and two female subjects (with their physical data listed in Table 4) were asked to flex and extend their upper arms to move the robot arm for five times consecutively, as illustrated in Figure 8. For comparison, the sets of CV_u and CV_l were obtained by both the trial and error method (Experiment 1) and the proposed ANFIS (Experiment 2). For Experiment 1, we made efforts to find proper CV_u and CV_l that achieved high discrimination rates for the four subjects, as listed in Table 5. The experimental results are shown in Figures 9-11. Figures 9-10 show the raw and filtered EMG signals for subjects A-D, respectively. Subject D exhibited higher fluctuations during flexion and extension, indicating that her skin impedance might be lower than those of others. Figure 11 shows the outputs from the classifier. The classification for these four subjects was in general successful, while one error detection at flexion was found for each of subjects B and C, and several doubtful ones for subject D. The SDR for each of them is 100%, 95.2%, 95.2% and 90.5%, respectively. It reveals that the system had detected some mutual muscle interferences during movements, and the low impedance of subject D affected the recording of EMG and consequently the classification.

Table 3. Mapping from EMG to robot movement.

EMG		Upper-arm Status	Classifier Output	Robot Arm
CH1	CH2			
OFF	OFF	Relaxation	0	STOP
ON	OFF	Flexion	1	UP
OFF	ON	Extension	2	DOWN
ON	ON	Error	3	STOP

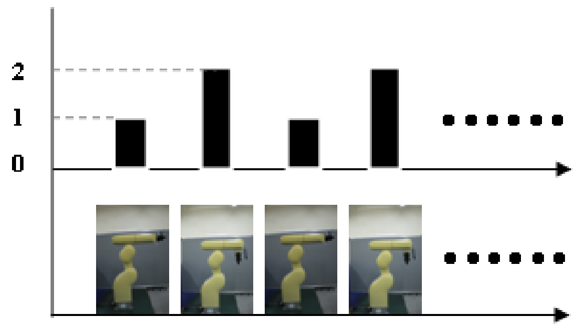

Figure 8. Robot arm movements corresponding to upper-arm movements.

Table 4. Physical data of the subjects.

Subject	Height (cm)	Weight (kg)	Gender	Muscle for electrode
A	166	60	Male	Slender
B	160	75	Male	Fat
C	155	52	Female	Ordinary
D	150	50	Female	Ordinary

Table 5. Critical values via the trial and error method.

Subject	CH 1		CH 2	
	CV_u	CV_l	CV_u	CV_l
A	4	2	3	2
B	3.2	1.5	3	2
C	4	3	5	4
D	3	2.5	3	2.5

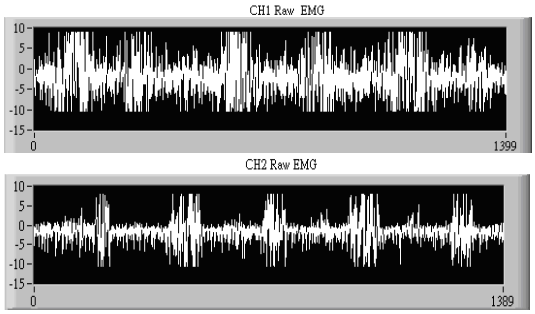

(a) subject A

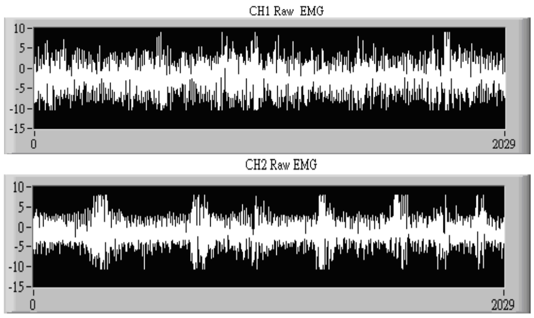

(b) subject B

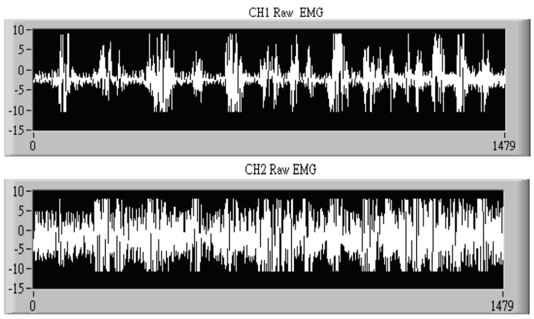

(c) subject C

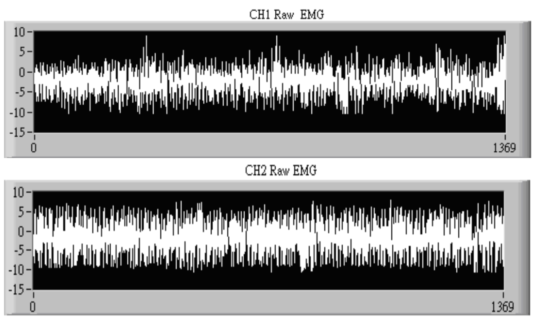

(d) subject D

Figure 9 Raw EMG signals for subject A-D in Experiment 1, upper CH1, lower CH2 (Horizontal coordinate: Time (sample), Vertical coordinate: Amplitude (voltage)).

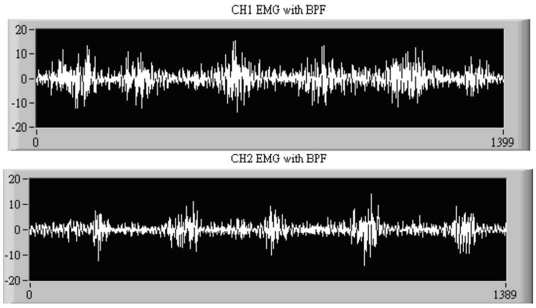

(a) subject A

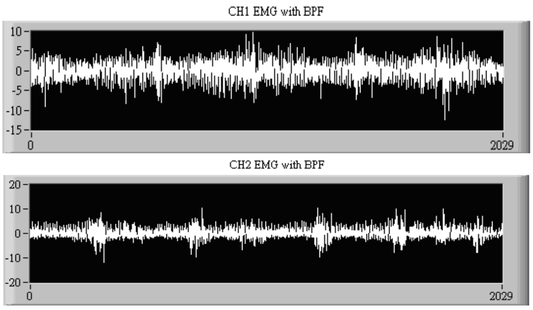

(b) subject B

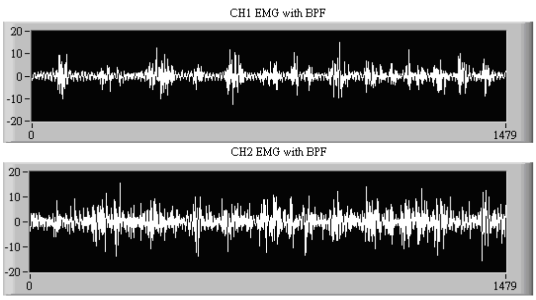

(c) subject C

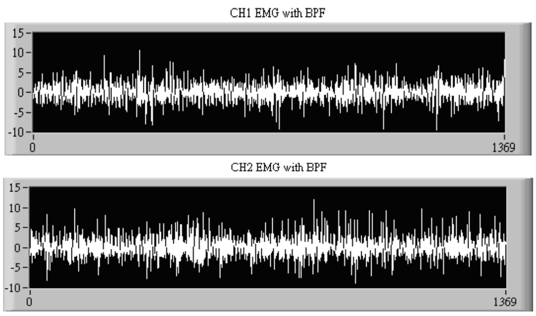

(d) subject D

Figure 10 Filtered EMG signals for subject A-D in Experiment 1 (Horizontal coordinate: Time (sample), Vertical coordinate: Amplitude (voltage)).

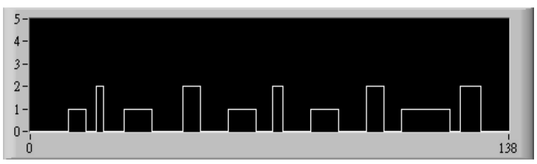

(a) subject A

(b) subject B

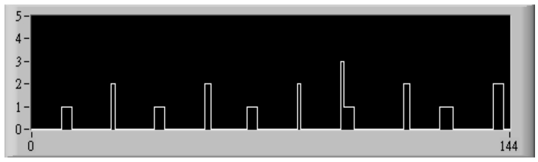

(c) subject C

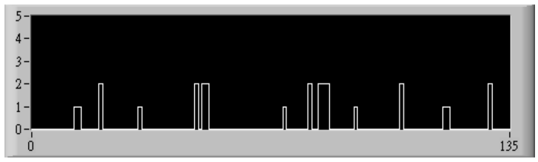

(d) subject D

Figure 11 Outputs from the classifier for subjects A-D in Experiment 1 (Horizontal coordinate: Time (second), Vertical coordinate: State (numbers 0-3 correspond to STOP, UP, DOWN, and ERROR, respectively)).

In Experiment 2, CV_u and CV_l were determined by the proposed ANFIS, as listed in Table 6. Figures 12-13 show the raw and filtered EMG signals, and Figure 14 the outputs from the classifier. The classification was very successful for all four subjects. The SDR is 100% for every subject. From classification results in Figures 11 and 14, CV_u and CV_l provided by the proposed ANFIS did achieve better performances than those by the trial and error method.

Table 6. Critical values via the proposed ANFIS.

Subject	CH 1		CH 2	
	CV_u	CV_l	CV_u	CV_l
A	3.34	2.51	2.51	2.44
B	3.29	2.46	3.27	2.46
C	2.59	1.94	4.14	3.1
D	3.47	2.6	4.19	3.15

4. Conclusions

This paper presents an adaptive upper-arm EMG-based robot control system. Via the ANFIS, the critical values for the initial point detection method adopted in the proposed system are determined. Experiments have been performed to demonstrate its effectiveness. In future works, we plan to apply the proposed system to govern arm motions with multiple degrees of freedom, in which close coupling between joints needs to be tackled.

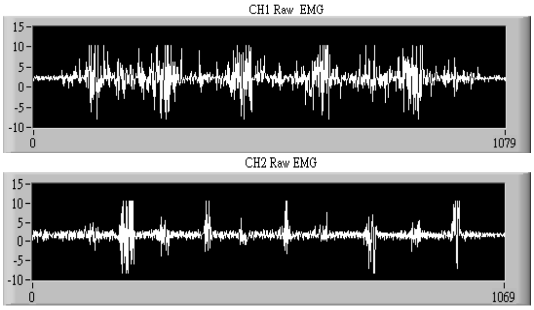

(a) subject A

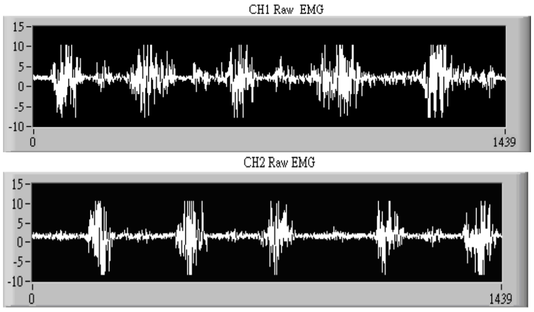

(b) subject B

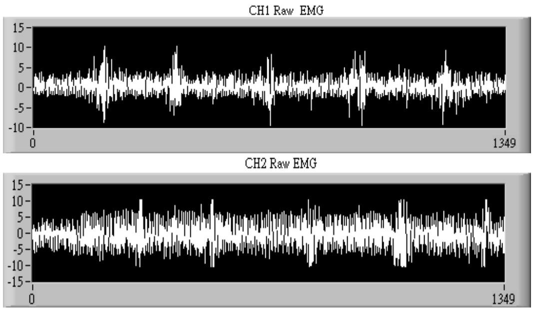

(c) subject C

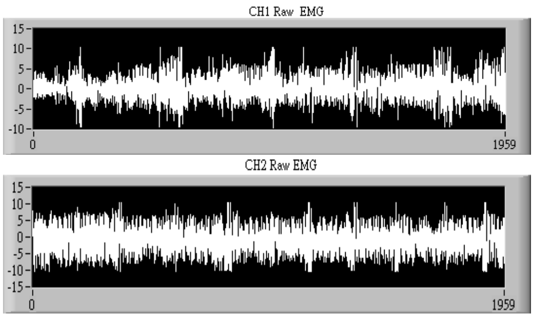

(d) subject D

Figure 12 Raw EMG signals for subject A-D in Experiment 2, upper CH1, lower CH2 (Horizontal coordinate: Time (sample), Vertical coordinate: Amplitude (voltage)).

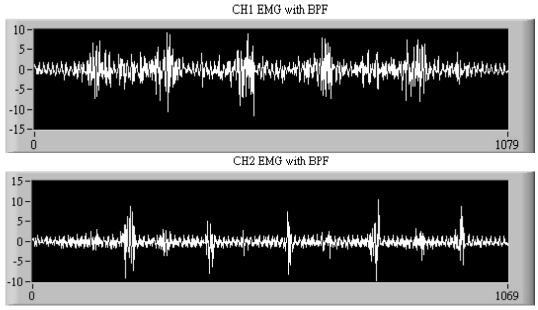

(a) subject A

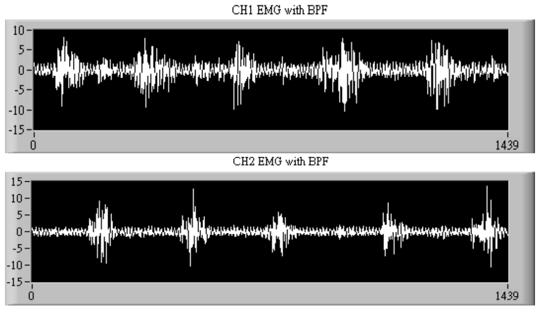

(b) subject B

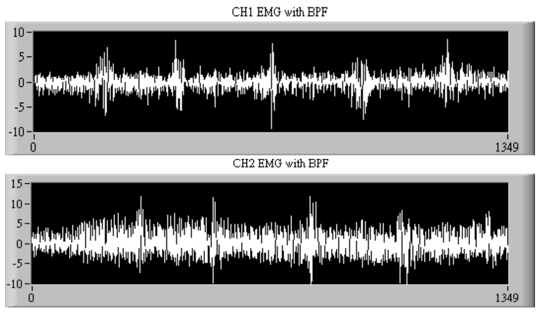

(c) subject C

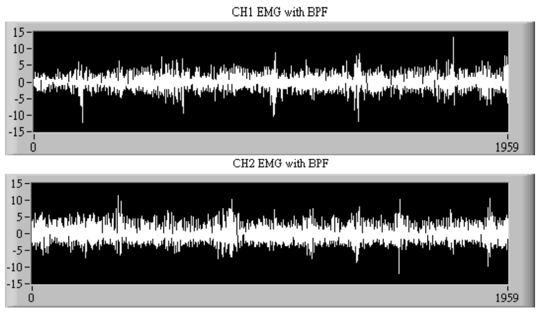

(d) subject D

Figure 13 Filtered EMG signals for subject A-D in Experiment 2 (Horizontal coordinate: Time (sample), Vertical coordinate: Amplitude (voltage)).

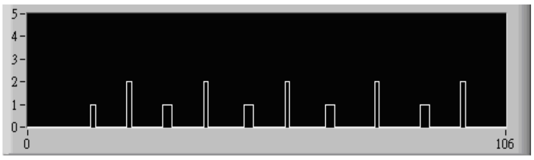

(a) subject A

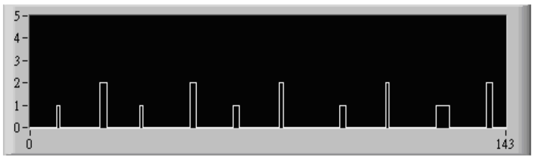

(b) subject B

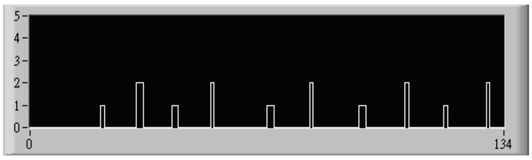

(c) subject C

(d) subject D

Figure 14 Outputs from the classifier for subjects A-D in Experiment 2 (Horizontal coordinate: Time (second), Vertical coordinate: State (numbers 0-3 correspond to STOP, UP, DOWN, and ERROR, respectively)).

Acknowledgment

This work was supported in part by the National Science Council under grant NSC 96-2628-E-009-164-MY3, and also Department of Industrial Technology under grants 97-EC-17-A-02-S1-032 and 98-EC-17-A-02-S2- 0047.

References

[1] K. Watanabe, C. Jayawardena, and K. Izumi, "Intelligent interface using natural voice and vision for supporting the acquisition of robot behaviors," *IEEE Conference on Sensors*, pp. 374-377, 2006.

[2] O. Fukuda, T. Tsuji, M. Kaneko, and A. Otsuka, "A human-assisting manipulator teleoperated by EMG signals and arm motions," *IEEE Transactions on Robotics and Automation*, vol. 19, no. 2, pp. 210-222, 2003.

[3] P. K. Artemiadis and K. J. Kyriakopoulos, "EMG-based position and force control of a robot arm: application to teleoperation and orthosis," *IEEE/ASME International Conference on Advanced Intelligent Mechatronics*, pp. 1-6, 2007.

[4] A. Ferreira, W. C. Celeste, F. A. Cheein, T. F. Bastos-Filho, M. Sarcinelli-Filho, and R. Carelli, "Human-machine interfaces based on EMG and EEG applied to robotic systems," *Journal of NeuroEngineering and Rehabilitation*, vol. 5, no. 10, pp. 1-15, 2008.

[5] Z. Gao, Q. Song, Y. Nie, J. Lei, Y. Yong, and Y. Ge, "Conceptual design and implementation of arm wrestling robot," *IEEE/RSJ International Conference of Intelligent Robots and Systems*, pp. 4582-4586, 2006.

[6] R. A. R. C. Gopura and K. Kiguchi, "EMG-based control of an exoskeleton robot for human forearm and wrist motion assist," *IEEE International Conference on Robotics and Automation*, pp. 731-736, 2008.

[7] P. Afshar and Y. Matsuoka, "Neural-based control of a robotic hand: evidence for distinct muscle strategies," *IEEE International Conference on Robotics and Automation*, pp. 4633-4638, 2004.

[8] N. Bu, M. Okamoto, and T. Tsuji, "A hybrid motion classification approach for EMG-based human-robot interfaces using Bayesian and neural networks," *IEEE Transactions on Robotics*, vol. 25, no. 3, pp. 502-511, 2009.

[9] H. J. Liu, P. C. Liu, and K. Y. Young, "Robot motion governing based on forearm EMG signals," *International Conference on Service and Interactive Robotics*, 2009.

[10] J. S. R. Jang, "ANFIS: adaptive network based fuzzy inference system," *IEEE Transactions on Systems, Man, and Cybernetics*, vol. 23, no. 3, pp. 665-683, 1993.

[11] B. K. Lee, K. H. Lee, and B. S. Chen, "State estimation of stochastic T-S fuzzy systems," *International Journal of Fuzzy Systems*, vol. 8, no. 1, pp. 46-56, 2006.

[12] C. Y. Kuo and H. F. Wang, "Overview of fuzzified neural networks with comparison of learning mechanism," *International Journal of Fuzzy Systems*, vol. 10, no. 2, pp. 71-80, 2008.

[13] M. J. Er, F. Liu, and M. B. Li, "Self-constructing fuzzy neural networks with extended Kalman filter," *International Journal of Fuzzy Systems*, vol. 12, no. 1, pp. 66-72, 2010.

[14] A. Subasi, "Application of adaptive neuro-fuzzy inference system for epileptic seizure detection using wavelet feature extraction," *Computers in Biology and Medicine*, vol. 37, no. 2, pp. 227-244, 2007.

[15] C. K. S. Vijila, P. Kanagasabapathy, S. Johnson, and V. Ewards, "Artifacts removal in EEG signal using adaptive neuro fuzzy inference system,"

IEEE International Conference Signal Processing, Communications and Networking, pp. 589-591, 2007.

[16] S. Micera, W. Jensen, F. Sepulveda, R. R. Riso, and T. Sinkjær, "Neuro-fuzzy extraction of angular information from muscle afferents for ankle control during standing in paraplegic subjects: an animal model," *IEEE Transactions on Biomedical Engineering*, vol. 48, no. 7, pp. 787-794, 2001.

[17] R. T. Lauer, B. T. Smith, and R. R. Betz, "Application of a neuro-fuzzy network for gait event detection using electromyography in the child with cerebral palsy," *IEEE Transactions on Biomedical Engineering*, vol. 52, no. 9, pp. 1532-1540, 2005.

[18] J. I. Park, J. H. Cho, M. G. Chun, and C. K. Song, "Neruo-fuzzy rule generation for backing up navigation of car-like mobile robots," *International Journal of Fuzzy Systems*, vol. 11, no. 1, pp. 192-201, 2009.

[19] M. Y. Shieh and K. H. Chang, "An optimized neuro-fuzzy controller design for bipedal locomotion," *International Journal of Fuzzy Systems*, vol. 11, no. 3, pp. 137-14, 2009.

Hsiu-Jen Liu received his B.S degree in Mechanical Engineering from National Taiwan University of Science and Technology, Taipei, Taiwan, R.O.C., in 1997, and M.S. degree in Aeronautics and Astronautics from National Cheng Kung University, Tainan, Taiwan, R.O.C., in 1999. He is currently working towards Ph.D. degree in Electrical and Control Engineering at National Chiao Tung University, Hsinchu, Taiwan, R.O.C. His academic interests include robot teleoperation, EMG signal processing and motion control.

Kuu-Young Young was born in Kaohsiung, Taiwan, 1961. He received his B.S. degree in Electrical Engineering from National Taiwan University, Taiwan, in 1983, and M.S. and Ph.D. degrees in Electrical Engineering from Northwestern University, Evanston, IL, U.S.A., in 1987 and 1990, respectively. Between 1983 and 1985, he served as an electronics officer in Taiwan Navy. Since 1990, he has been with the Department of Electrical Engineering at National Chiao-Tung University, Hsinchu, Taiwan, where he is currently a Professor. He served as the chairman of the department from 2003 to 2006, and the associate dean of Electrical and Computer Engineering College, NCTU, from 2007 to 2010. His research interests include robot compliance control, robot learning control, robot calibration and path planning, teleoperation, human machine interface, and Science, Technology, and Society (STS).